

# Cardiovascular System Modeling Using Windkessel Segmentation Model Based on Photoplethysmography Measurements of Fingers and Toes

## Abstract

**Background:** Photoplethysmography (PPG) contains information about the health condition of the heart and blood vessels. Cardiovascular system modeling using PPG signal measurements can represent, analyze, and predict the cardiovascular system. **Methods:** This study aims to make a cardiovascular system model using a Windkessel model by dividing the blood vessels into seven segments. This process involves the PPG signal of the fingertips and toes for further analysis to obtain the condition of the elasticity of the blood vessels as the main parameter. The method is to find the Resistance, Inductance, and Capacitance (RLC) value of each segment of the body through the equivalent equation between the electronic unit and the cardiovascular unit. The modeling made is focused on PPG parameters in the form of stiffness index, the time delay ( $\Delta t$ ), and augmentation index. **Results:** The results of the model simulation using PSpice were then compared with the results of measuring the PPG signal to analyze changes in the behavior of the PPG signal taken from ten healthy people with an average age of 46 years, compared to ten cardiac patients with an average age of 48 years. It is found that decreasing 20% of capacitance value and the arterial stiffness parameter will close to cardiac patients' data. Compared with the measurement results, the correlation of the PPG signal in the simulation model is more than 0.9. **Conclusions:** The proposed model is expected to be used in the early detection of arterial stiffness. It can also be used to study the dynamics of the cardiovascular system, including changes in blood flow velocity and blood pressure.

**Keywords:** Cardiovascular system, finger and toe photoplethysmography, photoplethysmography, stiffness index, Windkessel segmentation model

Submitted: 15-Mar-2021

Revised: 13-Feb-2022

Accepted: 22-Feb-2022

Published: 26-Jul-2022

## Introduction

Cardiovascular disease (CVD) is the leading cause of death in the world. Hypertension is clinically considered a significant factor in CVD. Hypertension is generally caused by age and lifestyle factors, such as smoking, consuming unhealthy food products, obesity, low physical activity, and alcohol consumption; these factors will then cause dysfunction in the endothelial layer. The endothelial layer under the arteries consists of a single layer of cells and elastic tissue, especially collagen. Endothelial dysfunction is a result of fat accumulation in the arteries, which causes the arteries to lose their elasticity. Those with hardening of the arteries are characterized by high blood pressure or hypertension.<sup>[1-4]</sup>

Electrocardiogram (ECG) device is usually used in monitoring cardiovascular health.

This is an open access journal, and articles are distributed under the terms of the Creative Commons Attribution-NonCommercial-ShareAlike 4.0 License, which allows others to remix, tweak, and build upon the work non-commercially, as long as appropriate credit is given and the new creations are licensed under the identical terms.

For reprints contact: WKHLRPMedknow\_reprints@wolterskluwer.com

Although ECG has been implemented through many improvements lately, users' flexibility, portability, and convenience are considered low.<sup>[5,6]</sup> The use of bio-electrodes attached to specific locations on the human body will reduce the flexibility and comfort of the user. Thus, photoplethysmography (PPG) emerged as an alternative measurement of heart rate monitors,<sup>[3]</sup> especially in measuring heart rate variability.<sup>[7]</sup>

PPG is a method of measuring blood circulation volume using an affordable and feasible optical instrument. PPG is often used to monitor heart rate with noninvasive technology using infrared rays and a photodetector on the surface of the skin. In addition, to show the approximate heart rate, the PPG signal contains some important information regarding human health conditions.<sup>[8]</sup> The PPG signal can be used to evaluate a variety of CVDs,

**How to cite this article:** Dewi EM, Hadiyoso S, Mengko TL, Zakaria H, Astami K. Cardiovascular system modeling using Windkessel segmentation model based on photoplethysmography measurements of fingers and toes. *J Med Sign Sens* 2022;12:192-201.

Ervin Masita Dewi<sup>1,2</sup>,  
Sugondo  
Hadiyoso<sup>1,3</sup>,  
Tati Latifah Erawati  
Rajab Mengko<sup>1</sup>,  
Hasballah Zakaria<sup>1</sup>,  
Kastam Astami<sup>1</sup>

<sup>1</sup>School of Electrical Engineering and Informatics, Institut Teknologi Bandung, Bandung, Indonesia, <sup>2</sup>Electrical Department, Politeknik Negeri Bandung, Bandung, Indonesia, <sup>3</sup>School of Applied Science, Telkom University, Bandung, Indonesia

## Address for correspondence:

Dr. Ervin Masita Dewi,  
School of Electrical Engineering and Informatics, Institut Teknologi Bandung, Bandung, Indonesia; Electrical Department, Politeknik Negeri Bandung, Bandung, Indonesia.  
E-mail: ervinmasita@polban.ac.id

## Access this article online

Website: [www.jmssjournal.net](http://www.jmssjournal.net)

DOI: 10.4103/jmss.jmss\_101\_21

## Quick Response Code:



including vascular stiffness, and the stiffness index (SI), as a parameter of vascular stiffness, can be analyzed for early detection of disease with potential soon.<sup>[9-11]</sup>

To study the cardiovascular system, it is necessary to make a mathematical model based on the anatomical and physiological data of an individual patient.<sup>[12-14]</sup> The model is a tool to simplify the real system so that its function can be better understood with the ultimate goal of making a medical device that is cheaper and more effective. One of the simple cardiovascular system models that can be used as decision support in clinical practice is the lumped parameter model. The cardiovascular system is modeled as a set of resistor (R), inductor (L), and capacitor (C) (electrical equivalent) circuits or modeled with the Windkessel (WK) model as an air chamber.<sup>[15-17]</sup>

The two-element WK model consists of R and C, which models the entire arterial system in terms of pressure and blood flow. Because it is very simple, this model cannot describe the propagation of the waves and their reflections that occur in body tissues.<sup>[18,19]</sup> The three-element WK model adds a resistor after the RC circuit as the impedance of the arterial system. The resistor acts as the total characteristic impedance, and the capacitor is stored to represent the elastic body tissue.<sup>[20,21]</sup> The addition of a resistor to the three-element WK significantly improves the accuracy of simulating systolic and diastolic pressures in the aorta.<sup>[22]</sup> Another WK-3 element model is to arrange the resistor and capacitor in series.<sup>[23]</sup> Both of these models cannot show wave reflection because of the elasticity of the blood vessel walls. To increase accuracy, WK-4 element was made by adding an inductor representing the inertia of the blood flow. The use of this inertia reduces the error of the input impedance.<sup>[24-27]</sup> The WK-2, WK-3, and WK-4 models have weaknesses in explaining the pressure from the venous side so that models with 5 and 6 elements are made, which provide a better description of the venous system.<sup>[28]</sup>

One-segment WK model that represents the entire vascular system is deemed insufficient to simulate the arterial system, so a multi-segmented model is made to represent the branches in the arteries. The blood vessels are divided into several segments and made as a series of R, L, and C, according to the characteristics of each segment.<sup>[29,30]</sup>

To the best of our knowledge, from several existing WK models, ranging from two elements to multi-compartment, there is no reflection on the diastolic part, and there is no simulation on the toes using PPG signal analysis. As it is known that blood is also pumped through the arteries

of the legs, therefore, in this study, a WK model with segmentation was analyzed to simulate PPG waves on the fingertips and toes to understand the reflection wave to the function of the cardiovascular system both upper and lower body vessels in a noninvasive manner. In this study, the cardiovascular system was modeled as an electrical circuit. This can express a distinct mechanical property of the blood vessels. In this study, blood vessels were modeled into seven segments which represent the main arteries in the human body. WK model is proposed with seven segments consisting of a series of R, L, and C. The parameters are arranged according to the classification of arterial segmentation. Segment-1 represents the fingertip, while segment-7 represents the toes. The heart is represented between segment-3 and segment-4. The other segments represent the blood vessels of the arms and legs. The determination of PPG signal parameters is done by comparing the PPG signal measured in healthy persons with the PPG signal measured in cardiac catheterization patients, which can be used as a supporting tool for early detection of CVD in the future.

## Materials and Methods

This research consists of two methodological stages. The first stage is the stage of collecting data used as reference data from the model by first conducting statistical tests (analysis of variance [ANOVA] test) to ensure that the data can be used as a reference. The second stage is the development of the WK segmentation model based on the physiology of blood vessels.

Several processes were carried out in collecting data, including PPG recording, signal preprocessing, and peak detection using first and second derivatives until the PPG parameter is obtained, as shown in Figure 1. In modeling the vascular system proposed in this study, modeling the WK circuit, which is equivalent to the vascular system. Figure 2 shows the proposed vascular modeling process.

### Data collection

This study analyzed PPG signals in healthy person and cardiac patient. Healthy adult subjects were selected with the criteria of having normal blood pressure and normal cholesterol. Meanwhile, cardiac patients were selected based on the criteria for patients who would undergo cardiac catheterization surgery. Subjects involved in the study were aged between 46 and 48 years. The number of samples involved in this study is based on the Slovin formula. With parameters, (1) the proportion of heart disease cases in Indonesia is 1.5%,<sup>[31,32]</sup> (2) the confidence



Figure 1: The stages in feature extraction of Photoplethysmography signal

level is 95%, and (3) alpha = 0.05. The data were collected from ten healthy persons and ten cardiac patients from Diagnostic and Cardiac Center Hasan Sadikin General Hospital Bandung recorded using noninvasive vascular analyzer (NIVA) device. NIVA is a noninvasive medical device with a pressure sensor and PPG sensor to analyze blood vessel health condition developed by the Biomedical Engineering Expertise Group, Bandung Institute of Technology. The person was measured while a person was lying down position so that heart and measured body part were in a parallel position. PPG sensor was placed at the fingertip and toes. The data recording was held for around 1 min, as seen in Figure 3.

### Photoplethysmography

The principle of the PPG sensor involves optical detection from blood volume change in a microvascular layer. PPG sensor monitors light intensity through the reflection or transmission from the light source, which emits through human skin tissue and then enters the light detector. The artery vessel contains a higher volume of blood in the systolic phase than in the diastolic phase. Figure 4 shows the measurement result of a healthy person using a PPG sensor in the NIVA device. The first peak shows that the systolic phase and the second peak indicates the diastolic phase, which is blood sent from the deflation process of the artery vessel wall.<sup>[33]</sup>

Figure 5 shows the PPG signal measured using NIVA at the tip of the little toe of a healthy person. In the second phase, the diastolic phase is not visible. This is because the distance between heart and toes is relatively farther than the distance between heart and fingertip.

Morphologically, the PPG signal could provide some information on the general condition of the blood vessel. Waveform arises from the pressure of the left ventricle to the fingertip, as shown in Figure 6.<sup>[3]</sup> The delay time ( $\Delta t$ ) is the time between the first peak, i.e., the systolic peak, and the second peak, i.e., the diastolic peak. The systolic peak is the moving-forward wave of the left ventricle, which moves directly to the fingertip. However, the diastolic peak arises from the deflation of the artery vessel and the left ventricle pressure transmitted to the lower part of the body and then reflected as a reflection wave to the fingertip, as seen in Figure 7.<sup>[3]</sup> The length of this path could be assumed as the proportional height of the persons.<sup>[10]</sup>

### Stiffness index

An objective assessment on the artery stiffness is crucial in the early detection of CVD. When the artery vessels get stiff, the bloodstream beneath will flow faster.<sup>[34,35]</sup> Artery stiffness could be assessed through PPG signal morphology; delay time ( $\Delta t$ ) between systolic peak and second peak or low diastolic peak indicates that there is already a stiffening artery. Based on Equation 1, it is known that the SI is comparable to subject height ( $H$ ) in centimeters proportionally and inversely proportional to delay time ( $\Delta t$ ) in seconds. The measurement unit of SI is cm/s.<sup>[36]</sup>

$$SI = \frac{H}{\Delta t} \tag{1}$$

Besides using the equations of SI, the assessment on the artery stiffness could also be analyzed through Equation 2 as augmentation index (AI), by comparing the height of systolic peak ( $x$ ) in mV to diastolic peak ( $y$ ) in mV.

$$AI = \frac{y}{x} \tag{2}$$

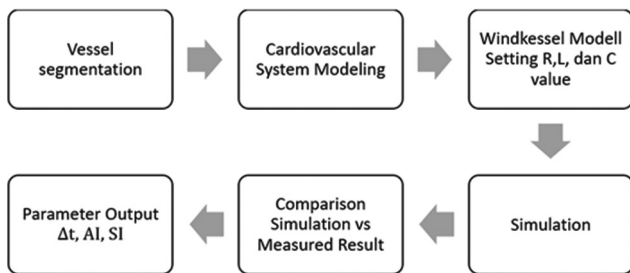


Figure 2: Proposed vascular modeling process



Figure 3: Recording fingertip and toe photoplethysmography signals using noninvasive vascular analyzer

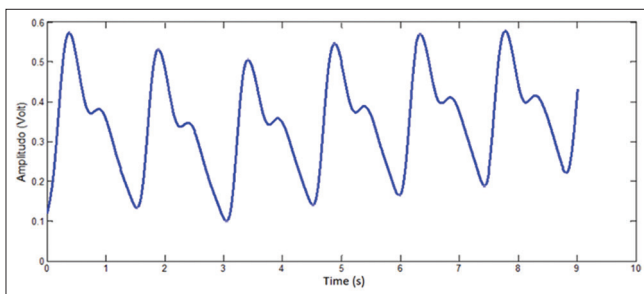


Figure 4: Fingertip photoplethysmography signal was taken by using noninvasive vascular analyzer

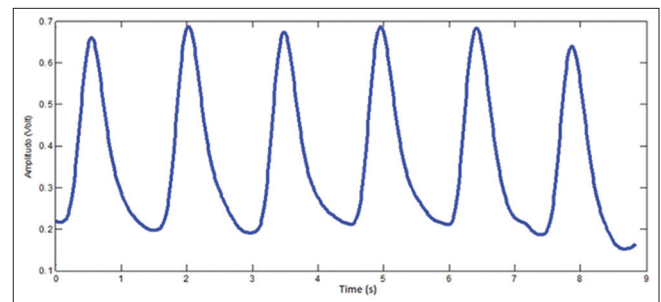


Figure 5: Toes photoplethysmography signal was taken by using noninvasive vascular analyzer

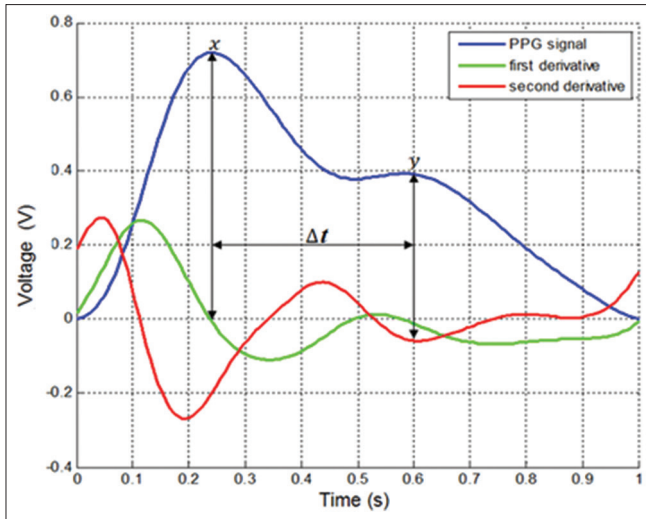


Figure 6: Sample morphology of photoplethysmography signal of healthy persons

To detect systolic and diastolic peaks using PPG signal, first and second derivative methods were used. The first derivative was used to obtain the peak of systolic, and the second derivative was used to obtain the peak of diastolic. This method is highly required since, in the case of the stiffness artery, the location of the diastolic peak is close to the systolic peak so that it could not be seen clearly. From Figure 5, the systolic peak is on the x axis, which is the intersection of the first derivative, while the diastolic peak is on the x axis, which is the second minimum peak of the second derivative.<sup>[37-40]</sup>

SI and AI are the functions of reflected waves affected by wave speed, as seen in Equation 3. In arteriosclerosis, transit time ( $\Delta t$ ) will decrease if the length of the track is ( $l$ ) similar in cm, then the wave speed ( $v$ ) in cm/s increases. From the Equation 4, with the vessel thickness ( $h$ ), the blood density ( $\rho$ ) in kg/m/s, and the vessel radius ( $r$ ) in cm, the modulus young ( $E$ ) in dyne/cm or the artery stiffness will increase if wave speed is increase.<sup>[24]</sup>

$$\Delta t = \frac{l}{v} \quad (3)$$

$$v = \sqrt{\frac{Eh}{2\rho r}} \quad (4)$$

### Windkessel model

Arteries system modeling is highly needed to assess the stiffness level of the artery vessel. WK model is a simple model of the blood circulation system that is illustrated in the form of electrical circuits. WK is derived from the German language that means air chamber. Otto Frank introduced the first WK model in 1899, and it was only made up of resistor (R) and capacitor (C).<sup>[41]</sup> In 1982, Buratini then added an inductor (L).<sup>[27,42,43]</sup> In 2007, Edmond Zaheldi concluded that the capacitor was closely related to artery stiffness, as written in Equation 5. Capacitor or

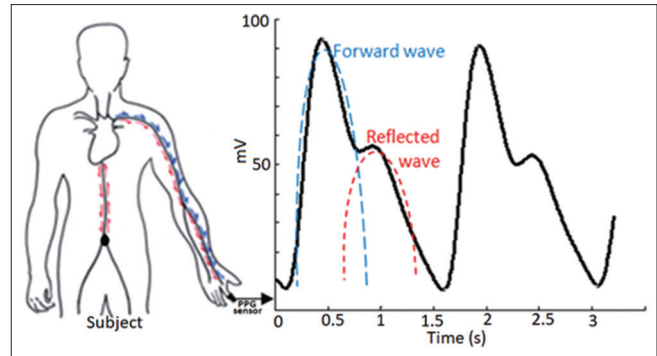


Figure 7: Forward and reflected waves on photoplethysmography signal

compliance ( $C$ ) is affected by blood volume ( $dv$ ) and blood pressure ( $dq$ ). In constant blood pressure, the capacitor depends on the blood volume, when the wall radius of artery vessels gets narrow due to the thickened artery wall that may cause vessel stiffness. Thus, the decrease in blood volume will lower the capacitance of the capacitor.<sup>[44,45]</sup>

$$C = \frac{dv}{dq} \quad (5)$$

This model equals to artery system with a hydraulic circuit, which consists of a pump, air chamber, and pipe. When the water is pumped, it will enter the chamber, and air in the chamber will press in entire directions. When there is no pressure from the pump, the pressure from the chamber will trigger the pipe's water flow. This principle is quite similar to the blood circulation system, where the heart functions as the pump that circulates blood to artery vessels as its channel. Artery vessels have similar elasticity and extensibility to the air chamber or an elastic reservoir. When the pump exerts pressure, the liquid will compress the air in the air chamber and when the pump stops, the liquid will still flow due to the compressed air. The same as blood vessels, it will release the pressure stored when the heart is pumping so that blood continues to flow when the heart is not pumping. In the electrical circuits, the heart is assumed as a voltage source that is connected to the diodes to generate half of the sinusoid signal. Vessels' elasticity and extensibility are illustrated as a capacitor which functions as a capacitor that, in the beginning, is used as charge retention that releases its charge when there is no flowing voltage. The resistor is illustrated as the obstacles of the pipe that is passed by the blood. Human blood vessel consists of a lot of segments and branches. The different diameter of each segment has caused different resistance value. The inductor is illustrated as the inertia of the bloodstream.<sup>[46]</sup>

WK model has a compliance or capacitor component that refers to the vessels' elasticity, extensibility, resistance, and inertia. The illustration of WK model can be seen in Figure 8a. The voltage source is AC wave with a frequency of 1.2 Hz that is in compliance with a heart period of around 0.8 s as a normal pulse for a healthy person. AC source is passing a diode to generate a signal with amplitude 150 mV



that is compatible with the heart signal that is half of the sinusoid signal. The heart signal was then passed through the RLC circuit. From the picture, three segments of R, L, and C circuits were used in the direction of fingers, resulting in the signal caught by fingers, as seen in Figure 8b.<sup>[47]</sup> This

segment modeled is only a bloodstream coming from the heart and passing to the subclavian artery, brachial artery, radial, and ulnar artery. The software used to simulate the model is Pspice from Cadence.

Simulation result of three-segment WK modeling can be seen in Figure 8b. The first line is the voltage source output and diodes that are illustrated with the heart signal. The second line is the output of the subclavian artery and the third line is the brachial artery, while the last is the radial and ulnar artery. In this model simulation, the last output does not show any reflection in the diastolic phase. Therefore, segments were then added for the lower part of body so that the reflection of diastolic phase was obtained as in the Figure 9.

## Results and Discussion

### Model simulations

The cardiovascular system model from 0D to 3D had been widely performed. It can be seen in the study on the cardiovascular model road map.<sup>[48]</sup> WK model or lump model or 0D model has been commonly used in a variety of fields on cardiovascular, from basic research on cardiovascular to the analysis of artificial cardiovascular. The full model of the blood circulation system and its parameter settings was simulated by using CeIIML language.<sup>[49]</sup> Meanwhile, any model with varying location and the amount of R, L,

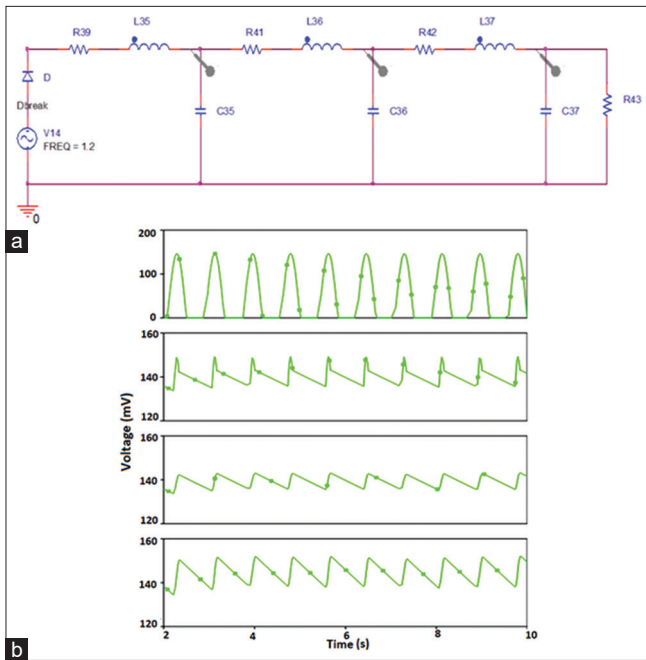


Figure 8: (a) Three-element Windkessel model, (b) result of model simulation

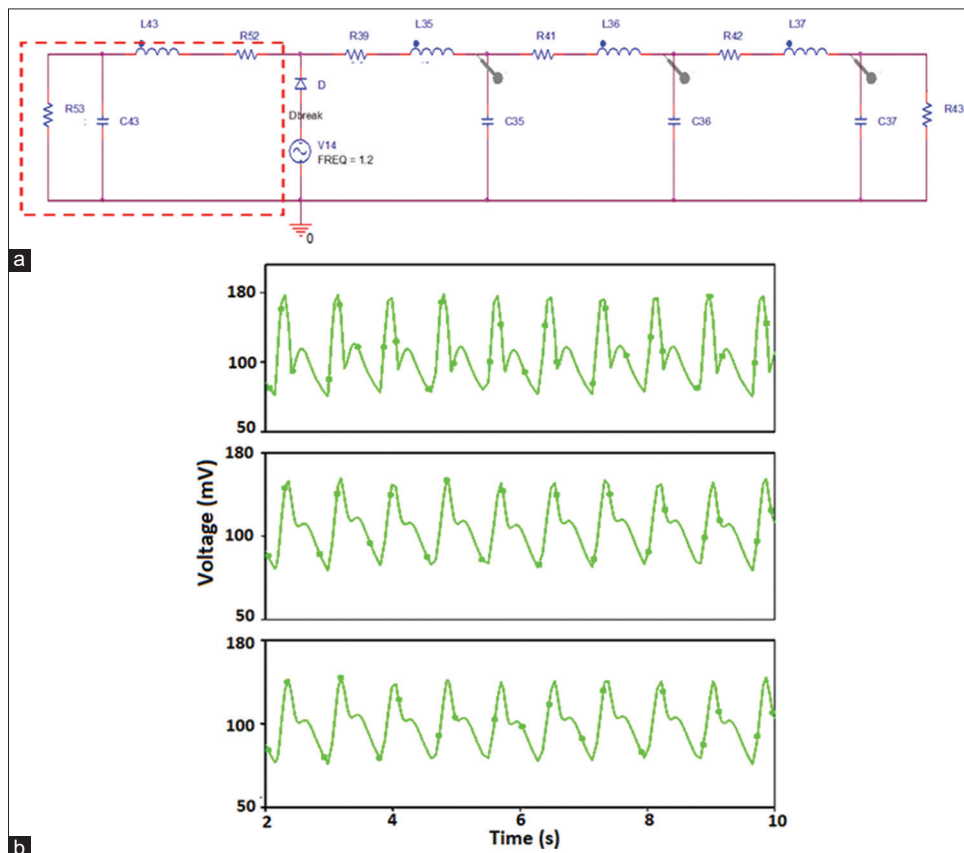


Figure 9: (a) Four segments Windkessel model, (b) result of model simulation

and C components or WK with three or four elements can be seen in several studies.<sup>[50]</sup> For the simulation of several WK models (WK-2, WK-3, and WK-4), there was no reflection seen in the diastolic part, and there has not been any simulation on toes based on PPG signal.

Therefore, this study created a WK model with segmentation to simulate PPG waves in fingertips and toes. The human body was classified into seven segments comprised three segments for the ventricle to the upper part of the body to fingers and four segments for the ventricle to the lower part of the body to feet. Each segment was three-element WK model, which consisted of R, L, and C circulation. The R component represents the resistance of the blood vessels, whose value depends on blood viscosity, radius, and vessel length. The L component is the inertia of blood flow, whose value depends on blood density, radius, and vessel length. The C component represents the storage in which the blood vessels will experience shrinkage and expansion according to the thickness of the walls of the vessels, modulus young, radius, and vessel length according to Equations 7 and 8. The equality relationship between the mechanical properties of the cardiovascular and electrical systems can be seen in Table 1,<sup>[51]</sup> while the values for R, L, and C obtained from the vessel physiological references can be seen in Table 2.

**Table 1: The equivalent table between electronic units and cardiovascular units**

| Cardiovascular unit     | Electronic parameter units      |
|-------------------------|---------------------------------|
| 0.01 ml/Pa              | 1 μF (compliance - capacitance) |
| 1 Pa.s <sup>2</sup> /ml | 1 μH (inertia - inductor)       |
| 1 Pa.s/ml               | 1 kΩ (resistance - resistance)  |
| Blood viscosity (μ)     | 1050 kg/m <sup>3</sup>          |
| Blood density (ρ)       | 0.0035 kg/m.s                   |

$$R = \frac{8\mu l}{\pi r^4} \tag{6}$$

$$L = \frac{9\rho l}{4\pi r^2} \tag{7}$$

$$C = \frac{3\pi r^3 l}{2Eh} \tag{8}$$

By entering the values of the components R, L, and C into the model and then simulating using PSipce as seen in Figure 10, the simulation results are obtained as seen in Figure 11. The blue color is the PPG signal on the fingertips, while the red color is the PPG signal on the toes. The shape of the signal has shown similarities to the PPG signal measured using NIVA. According to the American Heart Association standards for fingertips 120/80 mmHg and feet 168/112 mmHg for toes, there is a systolic phase and a diastolic phase.

**Photoplethysmography parameter measurement**

From the results of PPG wave measurements, waveform analysis was carried out so that the parameters of blood vessel stiffness were obtained. The parameters of vascular stiffness were obtained from the derivative results as shown in Table 3 for ten healthy people. The PPG parameter table for cardiac patients can be seen in Table 4. To find that the data have a significant difference in the measurement, ANOVA is used both in fingertips and toes with the results  $P < 0.05$  as shown in Table 5. It can be concluded that the data of healthy people and cardiac patients have significant differences so that further analysis can be carried out.

From the data of healthy people and cardiac patients, there are differences for all parameters of vessel stiffness.

**Table 2: Vessel segmentation, vessel physiological specification, and RLC values**

| Arterial segment number | Segment model | Anatomical components        | Length l (cm) | Radius r (cm) | Thickness h (cm) | Modulus young E (dyn/cm) | R (Ω)  | L (H)  | C (μF) |
|-------------------------|---------------|------------------------------|---------------|---------------|------------------|--------------------------|--------|--------|--------|
| 1                       | Fingertip     | Radial and ulnar artery      | 36.30         | 0.22          | 0.13             | 6.40                     | 1.57k  | 564.29 | 0.21   |
| 2                       |               | Brachial artery              | 20.80         | 0.32          | 0.06             | 4.00                     | 202.15 | 152.83 | 1.37   |
| 3                       |               | Subclavian artery            | 16.50         | 0.84          | 0.11             | 4.00                     | 3.46   | 17.81  | 10.67  |
| 4                       | Abdominal     | Torachid and abdominal aorta | 42.40         | 0.95          | 0.12             | 4.00                     | 5.31   | 35.35  | 36.97  |
| 5                       | Toe           | Iliac                        | 20.20         | 0.36          | 0.06             | 4.00                     | 122.56 | 117.27 | 1.80   |
| 6                       |               | Femoral artery               | 34.80         | 0.23          | 0.05             | 8.00                     | 1.34k  | 509.62 | 0.48   |
| 7                       |               | Tibial artery                | 41.90         | 0.13          | 0.07             | 13.00                    | 14.95k | 1.86k  | 0.04   |

RLC - Resistance, Inductance, and Capacitance

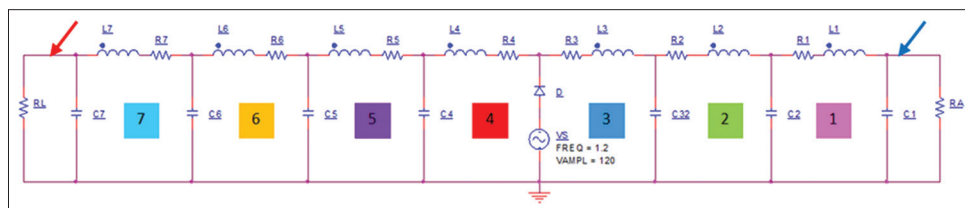


**Figure 10: Seven-segment arterial vessel modeling with the three-element Windkessel model**

**Table 3: Photoplethysmography parameter of the measurement result of 10 healthy persons**

| Age (years) | h (cm)    | PPG parameter on fingertip |           |           |           |              | PPG parameter on toes |           |           |           |              |
|-------------|-----------|----------------------------|-----------|-----------|-----------|--------------|-----------------------|-----------|-----------|-----------|--------------|
|             |           | x (mV)                     | y (mV)    | Dt (s)    | AI        | SI (cm/s)    | x (mV)                | y (mV)    | Dt (s)    | AI        | SI (cm/s)    |
| 36          | 173       | 2.45                       | 1.04      | 0.36      | 0.42      | 466.67       | 0.88                  | 0.07      | 0.63      | 0.07      | 274.60       |
| 64          | 152       | 3.85                       | 1.76      | 0.46      | 0.46      | 330.43       | 3.68                  | 0.24      | 0.50      | 0.06      | 304.00       |
| 45          | 152       | 4.62                       | 1.33      | 0.43      | 0.29      | 346.51       | 1.23                  | 0.06      | 0.72      | 0.05      | 211.11       |
| 43          | 154       | 3.89                       | 2.31      | 0.42      | 0.59      | 369.05       | 0.83                  | 0.05      | 0.53      | 0.05      | 290.57       |
| 41          | 142       | 5.94                       | 0.26      | 0.58      | 0.04      | 262.07       | 0.62                  | 0.05      | 0.66      | 0.07      | 215.15       |
| 33          | 149       | 2.58                       | 1.14      | 0.38      | 0.44      | 423.68       | 1.01                  | 0.13      | 0.42      | 0.13      | 354.76       |
| 62          | 155       | 3.12                       | 1.36      | 0.36      | 0.44      | 480.56       | 1.55                  | 0.04      | 0.58      | 0.02      | 267.24       |
| 50          | 161       | 3.47                       | 1.28      | 0.29      | 0.37      | 586.21       | 2.15                  | 0.07      | 0.61      | 0.03      | 263.93       |
| 48          | 168       | 5.16                       | 1.57      | 0.43      | 0.3       | 330.23       | 0.41                  | 0.03      | 0.67      | 0.07      | 250.75       |
| 40          | 170       | 5.46                       | 2.41      | 0.37      | 0.44      | 416.22       | 0.67                  | 0.04      | 0.67      | 0.05      | 253.73       |
| 46±10.22    | 158±10.06 | 4.05±1.21                  | 1.45±0.62 | 0.41±0.08 | 0.38±0.15 | 401.16±93.67 | 1.30±0.98             | 0.08±0.06 | 0.60±0.09 | 0.06±0.03 | 268.58±42.06 |

PPG - Photoplethysmography; SD - Standard deviation; SI - Stiffness index; AI - Augmentation index; Dt - The time delay

**Table 4: Photoplethysmography parameter of the measurement result of 10 cardiac patients**

| Patient | Age (years) | h (cm) | PPG parameter on fingertip |       |        |      |           | PPG parameter on toes |       |        |      |           |
|---------|-------------|--------|----------------------------|-------|--------|------|-----------|-----------------------|-------|--------|------|-----------|
|         |             |        | x (V)                      | y (V) | Dt (s) | AI   | SI (cm/s) | x (V)                 | y (V) | Dt (s) | AI   | SI (cm/s) |
| 1       | 47          | 154    | 1.85                       | 0.61  | 0.37   | 0.33 | 481.08    | 0.76                  | 0.22  | 0.46   | 0.29 | 334.78    |
| 2       | 45          | 178    | 2.82                       | 1.40  | 0.21   | 0.50 | 757.14    | 4.81                  | 0.56  | 0.41   | 0.11 | 434.15    |
| 3       | 58          | 149    | 2.64                       | 0.71  | 0.37   | 0.27 | 402.70    | 2.93                  | 0.36  | 0.48   | 0.12 | 310.42    |
| 4       | 48          | 159    | 2.98                       | 1.96  | 0.29   | 0.66 | 531.03    | 3.01                  | 0.45  | 0.52   | 0.15 | 305.77    |
| 5       | 51          | 150    | 2.54                       | 2.56  | 0.20   | 1.01 | 850.00    | 2.72                  | 0.55  | 0.46   | 0.20 | 326.09    |
| 6       | 55          | 170    | 3.26                       | 1.03  | 0.22   | 0.32 | 772.73    | 3.8                   | 0.61  | 0.42   | 0.16 | 404.76    |
| 7       | 51          | 167    | 3.41                       | 2.05  | 0.36   | 0.60 | 416.67    | 1.49                  | 0.18  | 0.52   | 0.12 | 321.15    |
| 8       | 38          | 148    | 5.76                       | 1.87  | 0.23   | 0.32 | 726.09    | 1.53                  | 0.27  | 0.56   | 0.17 | 264.29    |
| 9       | 56          | 159    | 3.55                       | 2.93  | 0.32   | 0.83 | 462.50    | 1.20                  | 0.16  | 0.43   | 0.13 | 369.77    |
| 10      | 33          | 170    | 8.04                       | 3.25  | 0.27   | 0.40 | 588.89    | 0.95                  | 0.21  | 0.43   | 0.22 | 395.35    |
| Mean    | 48          | 160    | 3.69                       | 1.84  | 0.28   | 0.52 | 598.88    | 2.32                  | 0.36  | 0.47   | 0.17 | 346.65    |
| SD      | 7.93        | 10.41  | 1.84                       | 0.91  | 0.07   | 0.25 | 164.45    | 1.34                  | 0.17  | 0.05   | 0.06 | 52.62     |

PPG - Photoplethysmography; SD - Standard deviation; SI - Stiffness index; AI - Augmentation index; Dt - The time delay

**Table 5: ANOVA test result**

|                  | F       | P       |
|------------------|---------|---------|
| <b>Fingertip</b> |         |         |
| Dt (s)           | 14.4451 | 0.0013* |
| AI               | 2.528   | 0.1293  |
| SI (cm/s)        | 10.9148 | 0.0039* |
| <b>Toes</b>      |         |         |
| Dt (s)           | 15.3358 | 0.0010* |
| AI               | 28.3002 | 0.0000* |
| SI (cm/s)        | 13.4309 | 0.0017* |

\*P<0.05. SI - Stiffness index; AI - Augmentation index; Dt - The time delay

This can be seen clearly in the picture of the average measurement results between healthy people and cardiac patients. A comparison PPG signal between healthy people and cardiac patients can be seen in Table 6. For fingertip, the mean signals can be seen in normal people, the second peak of fingertip PPG signal is clearly visible, whereas, in heart patients, the second peak of

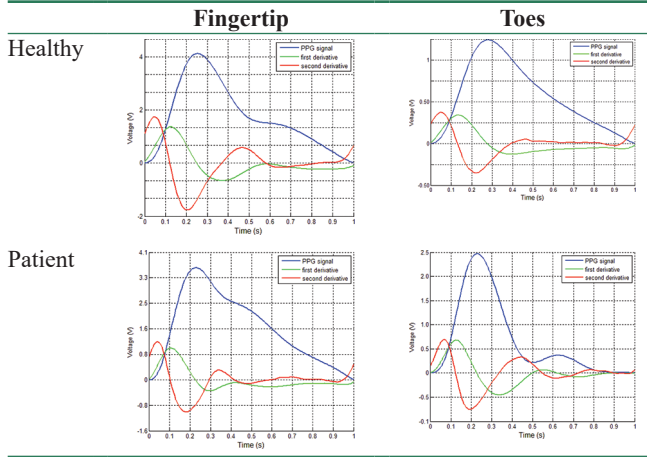
PPG signal is not clearly visible. After being analyzed using the second derivative, the value of the second peak of the PPG signal is obtained. The figure shows that the second peak for heart patients came earlier than the second peak for healthy people. From this, it can be concluded that the blood vessels of cardiac patients have decreased elasticity so that they appear earlier than healthy people.

At the tip of the toe, the PPG signal in the patient is seen as the reflection of the second peak is quite clear. From the patient's PPG signal, it was found that the AI was greater than the PPG signal in normal people and with smaller than normal people. The PPG signal at the tip of the toe does not have a reflected wave. The wave at the tip of the toe is a forward wave that is pumped from the heart without experiencing a reflection from the abdominal branches. Thus, to calculate the SI parameter, the estimation of the second peak wave (reflection result) is taken based on the delta time between the first peak and the second peak on the PPG fingertip.

### Photoplethysmography parameter simulation

Tables 7 and 8 show the results of the stiffness parameters of the model for fingertips and toes. Based on Equation 8, the smaller value of C, the value of Young's modulus ( $E$ ), which represents the value of elasticity, becomes increase. Increasing the value of E means that the strain value of the vessels is getting smaller, so it can be concluded that the blood vessels are stiff. Hence, in this research, the value of C was changed to obtain the parameters of arterial stiffness in the cardiac patient's model. Moreover, it is found that by reducing 20% of all C values, the parameter value of the model is close to the actual parameters. Using the Pearson's correlation method, the simulation result on this model has a high correlation  $r > 0.9$  which can be seen in Table 9.

**Table 6: Photoplethysmography signal comparison between healthy people and cardiac patients**



### Conclusions

This study has simulated a vascular model using an electric circuit with the WK approach. From this study, it can be concluded that the PPG signal of the fingertips and toes contains information on the health condition of blood vessels. Through PPG signal analysis, the stiffness of blood vessels can be determined as a reference for detecting CVD in the near future. Thus, a model of the arterial blood vessels of the human body's circulatory system can be constructed using measurement data. One simple model is the 0D model or lump model known as the WK model. This model uses an electric circuit with passive components consisting of R, L, and C components. R and L represent the magnitude of the PPG signal; meanwhile, C represents the elasticity of blood vessels. By dividing the arteries into

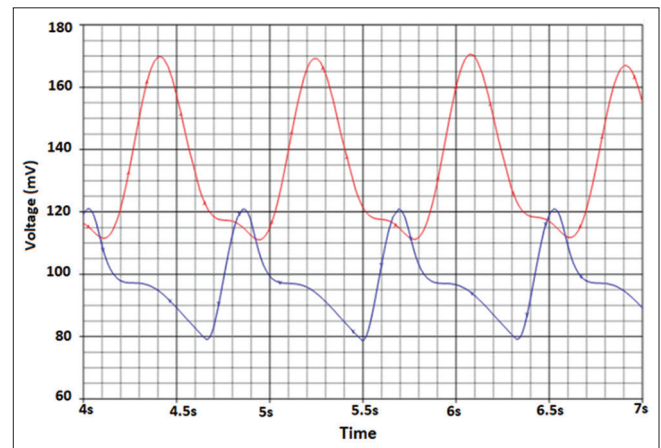


Figure 11: Windkessel segmentation simulation result

**Table 7: Photoplethysmography parameter of the measurement result of 10 healthy persons**

| PPG parameter | Fingertip  |              |        | Toes       |              |        |
|---------------|------------|--------------|--------|------------|--------------|--------|
|               | PPG signal | Output model | Derror | PPG signal | Output model | Derror |
| x (mV)        | 4.05±1.2   | 4.69         |        | 1.3±0.9    | 7.48         |        |
| y (mV)        | 1.45±0.6   | 1.87         |        | 0.08±0.06  | 0.52         |        |
| Dt (s)        | 0.41±0.08  | 0.44         | 0.07   | 0.60±0.09  | 0.56         | 0.07   |
| AI            | 0.38±0.15  | 0.40         | 0.05   | 0.06±0.03  | 0.07         | 0.16   |
| SI (cm/s)     | 401±93     | 365.71       | 0.09   | 268±42     | 288.23       | 0.07   |
| h (cm)        | 158±10     | 160          |        | 158±10     | 160          |        |

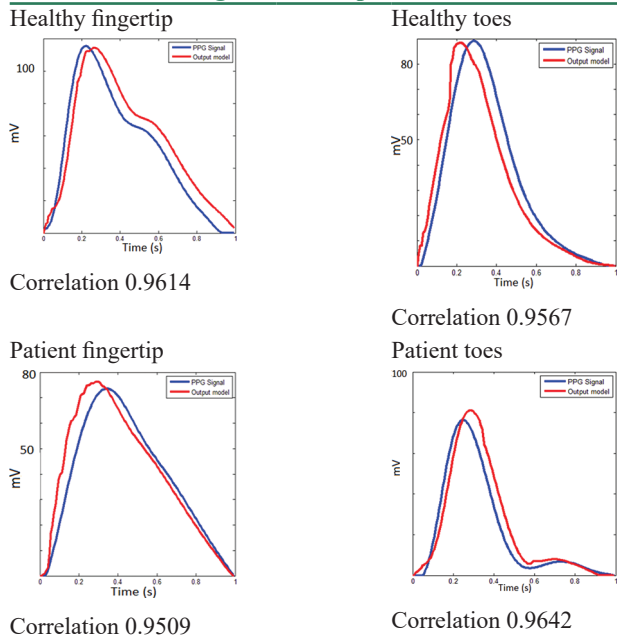
PPG - Photoplethysmography; SI - Stiffness index; AI - Augmentation index; Dt - The time delay

**Table 8: Photoplethysmography parameter of the measurement result of 10 patient**

| PPG parameter | Fingertip  |              |        | Toes       |              |        |
|---------------|------------|--------------|--------|------------|--------------|--------|
|               | PPG signal | Output model | Derror | PPG signal | Output model | Derror |
| x (mV)        | 3.69±1.8   | 5.76         |        | 2.32±1.3   | 10.30        |        |
| y (mV)        | 1.84±0.9   | 3.19         |        | 0.36±0.17  | 1.60         |        |
| Dt (s)        | 0.28±0.07  | 0.26         | 0.07   | 0.47±0.05  | 0.46         | 0.02   |
| AI            | 0.52±0.25  | 0.55         | 0.05   | 0.17±0.06  | 0.16         | 0.06   |
| SI (cm/s)     | 598±164    | 608.01       | 0.02   | 346±52     | 345.46       | 0.00   |
| h (cm)        | 160±10     | 160          |        | 160±10     | 160          |        |

PPG - Photoplethysmography; SI - Stiffness index; AI - Augmentation index; Dt - The time delay



**Table 9: Correlation between photoplethysmography signal and output model**

seven segments, a blood vessel simulation is created or what is commonly known as the WK segmentation model. This model can simulate the PPG measurement signal of fingers and toes with a correlation value above 0.9. From the developed model, it is found that there is a relationship between the capacitance value of the WK model and the vessel stiffness parameter. From this study, it is known that if the capacitance decreases by 20% will increase the risk of CVD. The WK model with this kind of segmentation is expected to be used in the early detection of arterial stiffness, and then, it can be used to study the dynamics of the cardiovascular system, including changes in blood flow velocity and blood pressure. The WK segmentation model is a simple model that is accurate in providing an approach to describe the cardiovascular system. However, in this modeling, the wave propagation in each segment has not been explained. For future improvements, other body segments can be added to make it more detailed, and another important thing is the comparison with patients with heart health disorders. Observations in the healthy group and the cardiac patient group need statistical tests and validation using a classification algorithm to determine the strength of the proposed modeling method. This study is expected to be used to complement the features of NIVA in predicting the pattern of wave flow in blood vessels.

### Acknowledgments

The authors would like to thank all those who have supported this study. Especially for biomedical laboratory crews who have assisted in PPG recording using NIVA. The authors also would like to thank the volunteers for participating in this study.

### Financial support and sponsorship

None.

### Conflicts of interest

There are no conflicts of interest.

### References

- Gaziano TA. Lifestyle and cardiovascular disease: More work to do. *J Am Coll Cardiol* 2017;69:1126-8.
- Riegel B, Moser DK, Buck HG, Dickson VV, Dunbar SB, Lee CS, et al. Self-care for the prevention and management of cardiovascular disease and stroke: A scientific statement for healthcare professionals from the American Heart Association. *J Am Heart Assoc* 2017;6:e006997.
- Dewi EM, Mengko TL, Zakaria H, Astami K. Increased arterial stiffness in characterization patient by photoplethysmography analysis. *International Conference on Electrical Engineering and Informatics*; 2019. Available from: <https://doi.org/10.1109/ICEEI47359.2019.8988783>. [Last accessed on 2020 Feb].
- Saveljik I, Nikolic D, Milosevic Z, Isailovic V, Nicolic M, Parodi O, et al. 3D modeling of plaque progression in the human coronary artery. *Proceedings* 2018;2:388.
- McLaughlin NB, Campbell RW, Murray A. Accuracy of four automatic QT measurement techniques in cardiac patients and healthy subjects. *Heart* 1996;76:422-6.
- Postema PG, De Jong JS, Van der Bilt IA, Wilde AA. Accurate electrocardiographic assessment of the QT interval: Teach the tangent. *Heart Rhythm* 2008;5:1015-8.
- Bolanos M, Nazeran H, Haltiwanger E. Comparison of heart rate variability signal features derived from electrocardiography and photoplethysmography in healthy individuals. *Conf Proc IEEE Eng Med Biol Soc* 2006;2006:4289-94.
- Zhang Z, Pi Z, Liu B. TROIKA: A general framework for heart rate monitoring using wrist-type photoplethysmographic signals during intensive physical exercise. *IEEE Trans Biomed Eng* 2015;62:522-31.
- Millasseau SC, Kelly RP, Ritter JM, Chowienzyk PJ. Determination of age-related increases in large artery stiffness by digital pulse contour analysis. *Clin Sci (Lond)* 2002;103:371-7.
- Elgendi M. On the analysis of fingertip photoplethysmogram signals. *Curr Cardiol Rev* 2012;8:14-25.
- Formaggia L, Lamponi D, Tuveri M, Veneziani A. Numerical modeling of 1D arterial networks coupled with a lumped parameters description of the heart. *Comput Methods Biomech Biomed Engin* 2006;9:273-88.
- Fu Y, Qiao A, Jin L. The influence of hemodynamics on the ulceration plaques of carotid artery stenosis. *J Mech Med Biol* 2015;15:1-14.
- Van de Vosse FN. Mathematical modelling of the cardiovascular system. *J Eng Math* 2003;47:175-83.
- Formaggia L, Quarteroni A, Veneziani A. Cardiovascular mathematics. In: *Modeling and Simulation of the Circulatory System*. Milan: Springer-Verlag; 2009.
- Heldt T, Mukkamala R, Moody GB, Mark RG. CVSim: An open-source cardiovascular simulator for teaching and research. *Open Pacing Electrophysiol Ther J* 2010;3:45-54.
- Shim EB, Sah JY, Youn CH. Mathematical modeling of cardiovascular system dynamics using a lumped parameter method. *Jpn J Physiol* 2004;54:545-53.
- Abdi M, Karimi A, Navidbakhsh M. A lumped parameter mathematical model to analyze the effects of tachycardia and

- bradycardia on the cardiovascular system. *Int J Numer Model Electron Netw Devices Fields* 2015;28:346-57.
18. Wetterer E. Flow and pressure in the arterial system, their hemodynamic relationship, and the principles of their measurement. *Minn Med* 1954;37:77-86.
  19. Westerhof N, Stergiopoulos N, Noble IM. *Snapshots of Hemodynamics an Aid for Clinical Research and Graduate Education*. 2<sup>nd</sup> ed. New York: Springer; 2010. Available from: <https://DOI:10.1007/978-1-4419-6363-5>. [Last accessed on 2020 Dec].
  20. Westerhof N, Bosman F, DeVries CJ, Noorder-Graaf A. Analogue studies of the human systemic arterial tree. *J Biomech* 1969;2:121-208.
  21. Westerhof N, Elzinga G, Sipkema P. An artificial arterial system for pumping hearts. *J Appl Physiol* 1971;31:776-81.
  22. Wang JJ, O'Brien AB, Shrive NG, Parker KH, Tyberg JV. Time-domain representation of ventricular-arterial coupling as a windkessel and wave system. *Am J Physiol Heart Circ Physiol* 2003;284:H1358-68.
  23. Burattini R, Natalucci S. Complex and frequency-dependent compliance of viscoelastic windkessel resolves contradictions in elastic windkessels. *Med Eng Phys* 1998;20:502-14.
  24. Stergiopoulos N, Westerhof BE, Westerhof N. Total arterial inertance as the fourth element of the windkessel model. *Am J Physiol* 1999;276:H81-8.
  25. Grant BJ, Paradowski LJ. Characterization of pulmonary arterial input impedance with lumped parameter models. *Am J Physiol* 1987;252:H585-93.
  26. Burattini R, Gnudi G. Computer identification of models for the arterial tree input impedance: Comparison between two new simple models and first experimental results. *Med Biol Eng Comput* 1982;20:134-44.
  27. Burattini R, Di Salvia PO. Development of systemic arterial mechanical properties from infancy to adulthood interpreted by four-element windkessel models. *J Appl Physiol* (1985) 2007;103:66-79.
  28. Frasch HF, Kresh JY, Noordergraaf A. Two-port analysis of microcirculation: An extension of windkessel. *Am J Physiol* 1996;270:H376-85.
  29. Milisic V, Quarteroni A. Analysis of lumped parameter models for blood flow simulations and their relation with 1D models. *Math Mod Numer Anal* 2004;38:613-32.
  30. Formaggia L, Veneziani A. *Reduced and Multiscale Models for the Human CVS*. Technical Report, PoliMI, Milan; 2003.
  31. Belarminus P, Florida Boa G. Factors affecting the occurrence of coronary heart disease in the general hospital of Waikabubak, Indonesia. *KnE Life Sci* 2022;2022:1004-12.
  32. Suryati T, Suyitno S. Prevalence and risk factors of the ischemic heart diseases in Indonesia: A data analysis of Indonesia basic health research (Risksdas) 2013. *Public Health Indonesia* 2020;6:138-44.
  33. Castaneda D, Esparza A, Ghamari M, Soltanpur C, Nazeran H. A review on wearable photoplethysmography sensors and their potential future applications in health care. *Int J Biosens Bioelectron* 2018;4:195-202.
  34. Bramwell JC, Hill A. Velocity of transmission of the pulse-wave. *Lancet* 1922;199:891-2.
  35. Eliakim M, Sapoznikov D, Weinman J. Pulse wave velocity in healthy subjects and in patients with various disease states. *Am Heart J* 1971;82:448-57.
  36. Elgendi M, Fletcher R, Liang Y, Howard N, Lovell NH, Abbott D, *et al.* The use of photoplethysmography for assessing hypertension. *NPJ Digit Med* 2019;2:60.
  37. Simek J, Wichterle D, Melenovsky V, Malik J, Svacina S, Widimsky J. Second derivative of the finger arterial pressure waveform: An insight into dynamics of the peripheral arterial pressure pulse. *Physiol Res* 2005;54:505-13.
  38. Millasseau SC, Guigui FG, Prasa J, Cockcroft JR, Ritter JM, Choweienzyk PJ. Non-invasive assessment of the digital volume pulse comparison with the peripheral pressure pulse. *Hypertension* 2000;36:952-7.
  39. Elgendi M, Norton I, Brearley M, Abbott D, Schuurmans D. Systolic peak detection in acceleration photoplethysmograms measured from emergency responders in tropical conditions. *PLoS ONE* 2013;8:e76585.
  40. Yousef Q. Assessment of atherosclerosis in erectile dysfunction subjects using second derivative of photoplethysmogram. *Sci Res Essays* 2012;7:2230-6.
  41. Olufsen MS, Nadim A. On deriving lumped models for blood flow and pressure in the systemic arteries. *Math Biosci Eng* 2004;1:61-80.
  42. Palladino JL, Ribeiro LC, Noordergraaf A. Human circulatory system model based on Frank's mechanism. *Stud Health Technol Inform* 2000;71:29-40.
  43. Zahedi E, Chellappan K, Ali MA, Singh H. Analysis of the effect of ageing on rising edge characteristics of the photoplethysmogram using a modified Windkessel model. *Cardiovasc Eng* 2007;7:172-81.
  44. Allen J, Murray A. Modelling the relationship between peripheral blood pressure and blood volume pulses using linear and neural network system identification techniques. *Physiol Meas* 1999;20:287-301.
  45. Catanho M, Sinha M, Vijayan V. *Model of Aortic Blood Flow Using the Windkessel*. *Mathematical Methods in Bioengineering Report*; 2012. p. 1-15.
  46. Ferreira A, Souza M. Three-section transmission-line arterial model for non-invasive assessment of vascular remodeling in primary hypertension. *Biomed Signal Process Control* 2009;4:2-6.
  47. Safaei S, Bradley CP, Suresh V, Mithraratne K, Muller A, Ho H, *et al.* Roadmap for cardiovascular circulation model. *J Physiol* 2016;594:6909-28.
  48. Shi Y, Lawford P, Hose R. Review of zero-D and 1-D models of blood flow in the cardiovascular system. *Biomed Eng Online* 2011;10:33.
  49. Deepankaew R, Naiyanetr P. *The Simulation of Cardiovascular System for Physiology Study*. The 7<sup>th</sup> Biomedical Engineering International Conference; 2014. Available from: <https://DOI:10.1109/BMEiCON.2014.7017430>. [Last accessed on 2020 Dec].
  50. Avolio AP. Multi-branched model of the human arterial system. *Med Biol Eng Comput* 1980;18:709-18.
  51. Ghasemalizadeh O, Mirzaee M, Firoozabadi B. Modeling the human cardiovascular system and peristaltic motion of descending arteries using the lumped method. *Internet J Bioeng* 2012;3:1-11.